AFWAL-TR-89-4003

INFLUENCE OF TEMPERATURE ON THE LOW CYCLE FATIGUE OF SURFACE MOUNTED CHIP CARRIER/PRINTED WIRING BOARD JOINTS

H.D. Solomon

Materials Laboratory

Martin Marietta Corporation
Orlando, FLA 32855-5837

September 1987

Interim Report

MATERIALS LABORATORY
AIR FORCE WRIGHT AERONAUTICAL LABORATORIES
AIR FORCE SYSTEMS COMMAND
WRIGHT-PATTERSON AIR FORCE BASE, OHIO 45433-6533

Unclassified
SECURITY CLASSIFICATION OF THIS PAGE

ADA204336

REPORT DOCUMENTATION PAGE

Form Approved
OMB No. 0704-0188

1a. REPORT SECURITY CLASSIFICATION Unclassified	1b. RESTRICTIVE MARKINGS
2a. SECURITY CLASSIFICATION AUTHORITY None	3. DISTRIBUTION/AVAILABILITY OF REPORT Approved for Public Release; Distribution Unlimited
2b. DECLASSIFICATION/DOWNGRADING SCHEDULE None	
4. PERFORMING ORGANIZATION REPORT NUMBER(S) 87CRD186	5. MONITORING ORGANIZATION REPORT NUMBER(S) AFWAL-TR-89-4003
6a. NAME OF PERFORMING ORGANIZATION Martin Marietta Corp. 6b. OFFICE SYMBOL (If applicable)	7a. NAME OF MONITORING ORGANIZATION Materials Laboratory (AFWAL/MLTE) Air Force Wright Aeronautical Laboratories
6c. ADDRESS (City, State, and ZIP Code) P.O. Box 5837, Orlando, Florida 32855-5837	7b. ADDRESS (City, State, and ZIP Code) Wright-Patterson AFB, OH 45433-6533
8a. NAME OF FUNDING/SPONSORING ORGANIZATION Materials Laboratory 8b. OFFICE SYMBOL (If applicable)	9. PROCUREMENT INSTRUMENT IDENTIFICATION NUMBER F33615-85-C-5065
8c. ADDRESS (City, State, and ZIP Code) Air Force Wright Aeronautical Laboratories Wright-Patterson AFB, OH 45433-6533	10. SOURCE OF FUNDING NUMBERS PROGRAM ELEMENT NO. 78011F; PROJECT NO. 3095; TASK NO. 04; WORK UNIT ACCESSION NO. 02

11. TITLE (Include Security Classification)
Influence of Temperature on the Low Cycle Fatigue of Surface Mounted Chip Carrier/Printed Wiring Board Joints

12. PERSONAL AUTHOR(S)
Solomon, H.D.

13a. TYPE OF REPORT	13b. TIME COVERED	14. DATE OF REPORT (Year, Month, Day)	15. PAGE COUNT
Interim	FROM _____ TO _____	September 1987	28

16. SUPPLEMENTARY NOTATION

17. COSATI CODES		
FIELD	GROUP	SUB-GROUP
20	11	

18. SUBJECT TERMS (Continue on reverse if necessary and identify by block number)
surface mount technology, chip carrier, PWB, low cycle fatigue, joint cracking

19. ABSTRACT (Continue on reverse if necessary and identify by block number)

This is a study of the Low Cycle Fatigue of Chip Carrier/Printed Wiring Board joints tested at -55°C and +125°C. It differs from a previous study where the joints were tested at 35°C. The hysteresis loops were distorted. The slopes of the displacement vs. fatigue life curves were slightly lower and the fatigue lives were longer. These differences were especially significant when the change in joint resistance was used to define failure.

20. DISTRIBUTION/AVAILABILITY OF ABSTRACT ☒ UNCLASSIFIED/UNLIMITED ☐ SAME AS RPT. ☐ DTIC USERS	21. ABSTRACT SECURITY CLASSIFICATION Unclassified
22a. NAME OF RESPONSIBLE INDIVIDUAL Preston Opt	22b. TELEPHONE (Include Area Code) (513) 255-2461 22c. OFFICE SYMBOL AFWAL/MLTE

DD Form 1473, JUN 86 *Previous editions are obsolete.* SECURITY CLASSIFICATION OF THIS PAGE

INFLUENCE OF TEMPERATURE ON THE LOW CYCLE FATIGUE OF SURFACE MOUNTED CHIP CARRIER/PRINTED WIRING BOARD JOINTS

H.D. Solomon

1. INTRODUCTION

The low cycle fatigue, at 35 °C, of surface mounted chip carrier/printed wiring board joints was considered in a previous study [1], from here on denoted as [1]. This study has been expanded to consider the low cycle fatigue (LCF) at -55 °C and + 125 °C, and this behavior is contrasted with that previously observed at 35 °C. This extension to -55 °C and + 125 °C was necessitated by the fact that thermal fatigue over this temperature range is a primary life-limiting factor in leadless chip carrier(CC)/printed wiring board (PWB) joints. Without a lead to flex in response to thermal strains, the solder joint can be subjected to large strains, which will result in fatigue failure. This study, like the previous one conducted at 35 °C, utilizes mechanical strains at a constant temperature to induce failure. This mechanical cycling was done on actual CC/PWB joints. The present study utilizes the same experiment equipment run in the same manner, except that the cycling was done at -55 °C or + 125 °C.

2. EXPERIMENTAL PROCEDURES

Since the details of the experimental procedures are given in [1], only a brief review will be given here. Two sides of a 44IO chip carrier were soldered to a glass polyimide PWB and the assembly mounted into a testing machine, as shown in Figure 1. After assembly in the testing machine, the PWB is cut in half by extending the slots shown in Figure 1. When the load is applied it will now be carried solely by the solder joints. Extensometers are attached across each row of joints so that the displacement of each row can be measured separately on each cycle and summed with an analog computer. The load being applied for a fixed control displacement is also monitored on every cycle.

The specimen is contained within a box which is filled with flowing N_2, primarily to prevent ice formation at -55 °C. Liquid nitrogen and a heater are used to achieve the desired temperature, which is kept at 125 °C ± 0.5 °C or -55 °C ± 1 °C throughout the test.

The circuit on the PWB is used to measure the voltage drop through the solder joint. Periodically throughout the fatigue cycling, the test was stopped and the resistance of each joint measured individually and sequentially.

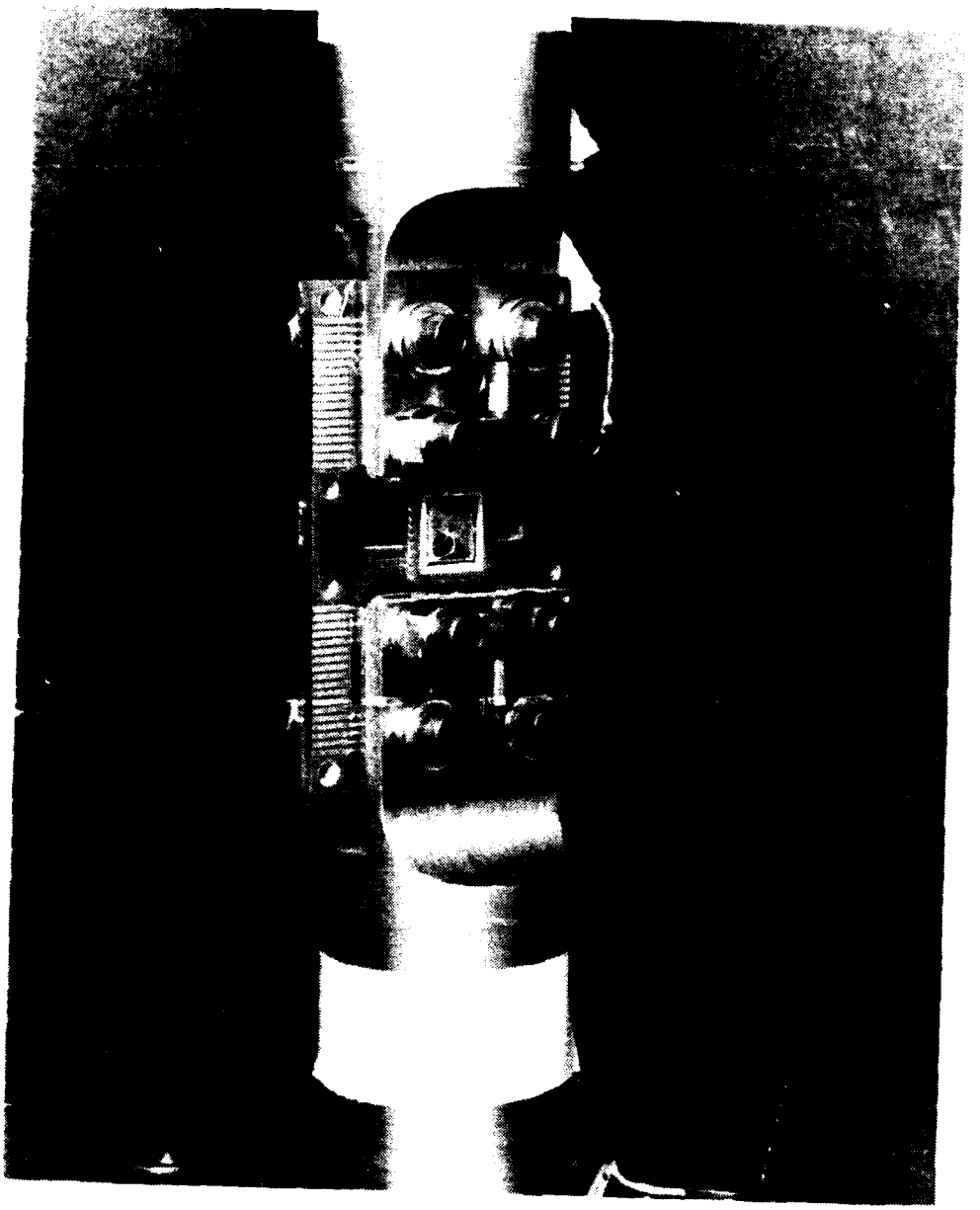

Figure 1. Test specimen assembly.

The tests were run by applying various *shear* plastic displacements to the joints. The plastic displacement was determined with an analog plastic strain computer which subtracted out the elastic displacement of the solder and test fixture. The crosshead was reversed at predetermined plastic displacement limits with the + plastic displacement limit equal to the absolute value of the negative limit. Since the tests were in shear, the + and - limits do not represent tensile or compressive displacement, but rather first shearing in the opposite directions. The + and - signs denote the sign of the load signal measured by the load cell.

The cycling limits were determined from the sum of the displacements for the top plus bottom rows of joints. While the control was not done on the basis of the displacement of the individual rows of joints, these displacements were continuously recorded. See [1] for more details.

3. EXPERIMENTAL RESULTS

The fatigue cycling produced the hysteresis loops of the sort shown in Figures 2 and 3. Three different types of loops are shown. The load is shown vs. (a) displacement of the top plus bottom rows of joints, (b) the plastic displacement determined from a, and (c) the individual displacements of the top and bottom rows of joints. The hysteresis loops are shown at the start of the test and after the load has dropped by about 90%. Several different types of displacements are defined in the figures and will be employed in subsequent figures. The displacement Δ_p is the plastic component of the top plus bottom displacements, as measured at the crosshead reversals. The displacement can also be measured at zero load as is done (i.e., Δ_{ps}) for displacement of the single row of top or bottom joints, or for the sum of the top and bottom rows, i.e., Δ_{pz} .

Figures 2 and 3 illustrate that the elastic slopes of the displacements measured on the top and bottom rows of joints are not exactly the same. This stems from differences in the joint geometries and from a small degree of bending. Even with the solder joint at the load line and the specimen loaded inside a split grip, some bending is naturally induced because the chip carrier and PWB cannot both be exactly positioned along the load line. Furthermore, this bending is not exactly the same for the top and bottom rows of joints, giving rise to differences in the compliance of the individual joint rows. These differences largely cancelled out, however, when the individual displacements are summed to give Δ_p, which varies by only less than 10% from one test to another. This bending of each row of joints is much less than that measured with other gripping systems [1], where employed. In these early tests, a net (for the sum of the rows of joints) bending angle as large as 10^{-3} deg/lb was noted, but this small net bending did not reduce the fatigue life.

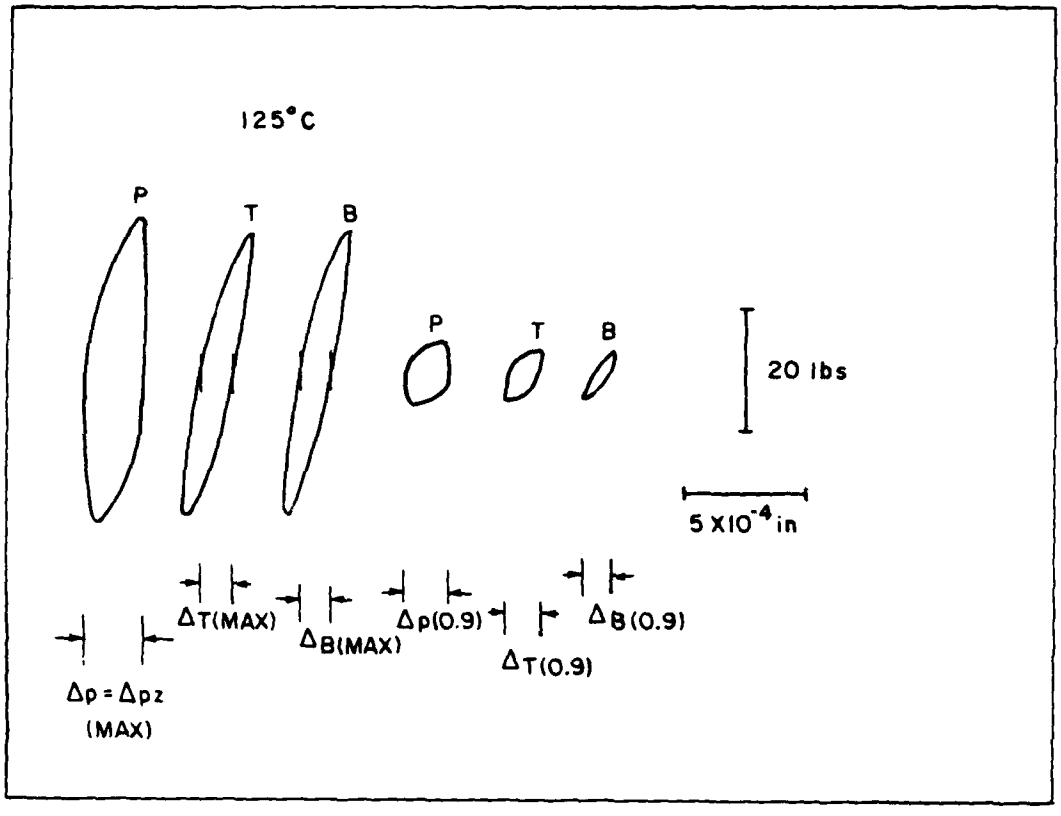

Figure 2. Hysteresis loops generated at 125 °C.

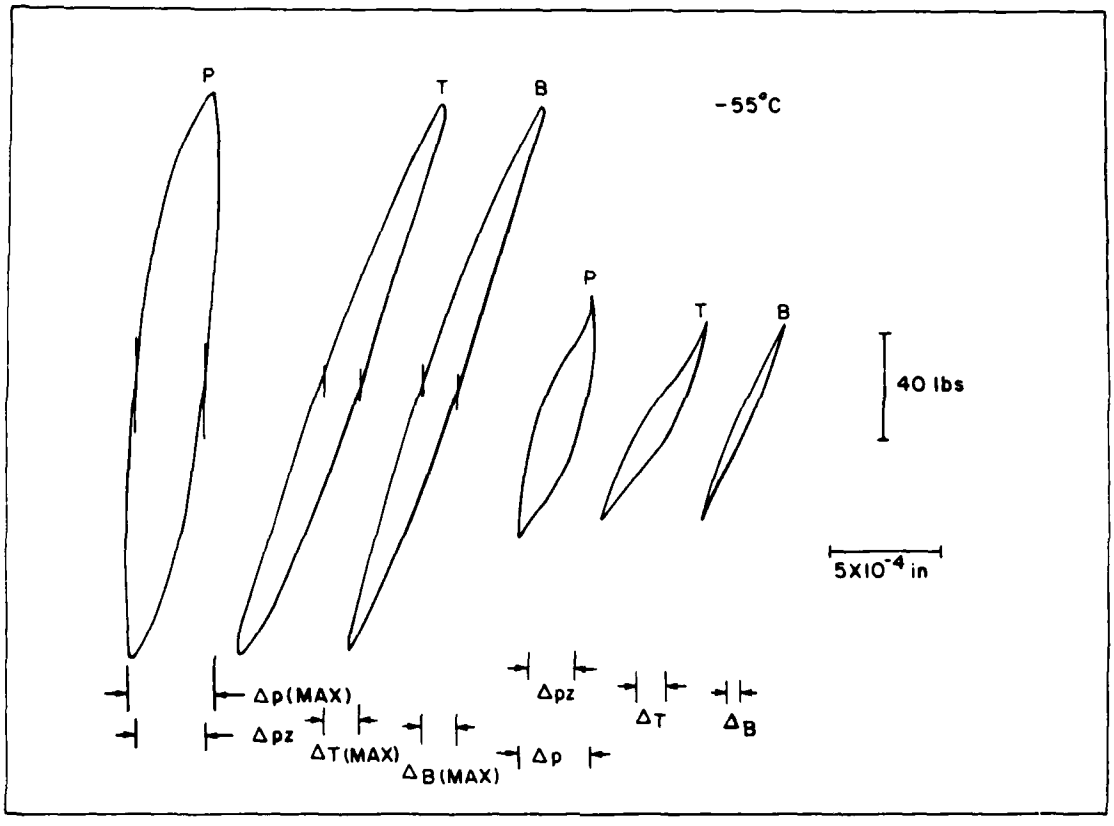

Figure 3. Hysteresis loops generated at -55 °C.

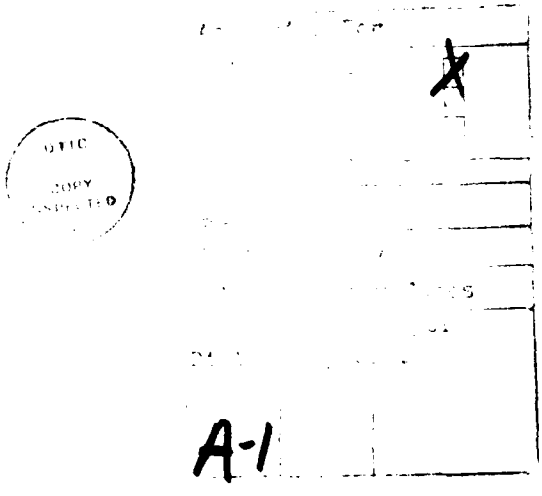

As the test progresses and the load drops, the net compliance (measured with both rows of joints) increases because fatigue cracking has decreased the load bearing area. Unfortunately, the plastic strain computer was set for the initial compliance and was not changed throughout the test. Thus, even though the plastic displacement limit was fixed, the measured plastic displacement, Δ_p, decreased somewhat throughout the test because its determination depends on the compliance. It was therefore necessary to measure this displacement at various intervals during the experiment. The appelation max as in $\Delta_{p\,(max)}$ or $\Delta_{ps\,(max)}$ refers to displacements measured as close as possible to the cycle exhibiting the maximum load range. (Since these hysteresis loops were measured individually on an x-y recorder, only one type of loop could be measured on any given cycle, so it was not possible to measure every hysteresis at the max load). The displacements were also recorded after a load drop of 50% and 90%.

The compliance changes not only reduce Δ_p , they also alter the hysteresis loop shape. At the start of the test, the elastic unloading continues to zero load and Δ_p measured at zero load (except at -55 °C) is the same as that measured at the crosshead reversals. At -55 °C the hysteresis loops are not completely symmetric, and Δ_p measured at zero load is a little less than that measured at the crosshead reversal (see Figure 3). By a 50% drop in load, changes in the compliance alter the elastic unloading enough to make Δ_p measured at zero load (Δ_{pz}) less than Δ_p at all the temperatures [1]. By a 90% drop in load, this effect becomes pronounced especially at -55 °C (see Figure 3). This effect necessitates considering the fatigue life not only in terms of Δ_p, but also in terms of Δ_{pz}. These effects will be discussed.

The hysteresis loop distortions, evident at -55 °C, result from joint misalignments and the higher strength of the solder at this temperature. This causes the imposed displacement to be taken up in joint bending and chip carrier deflection rather than by as much joint deformation as it is at the higher temperatures. Since one leg of each extensometer measures the displacement across the top and bottom rows of joints, chip carrier deflections will cause complementary distortion in the hysteresis loops drawn from the top and bottom row of displacements. These complementary distortions are illustrated in Figure 3. Fatigue cracking causes further misalignments and more hysteresis loop distortions. This bending, which is different on loading and unloading on each row, causes Δ_{pz} to be considerably smaller than Δ_p. This is especially true at the lower displacements where the joint plastic deformation is less and can be overshadowed by the bending.

As can be seen in Figures 2 and 3, reducing the temperature increases the load required to develop a given displacement. The hysteresis load range is shown vs. $\Delta_{p\,(max)}$, in Figure 4 for the -55 °C and + 125 °C tests as compared to the results obtained at 35 °C. In addition to the differences in load range, there are differences in the shapes of the 125 °C and -55 °C hysteresis loops which are discussed in the next

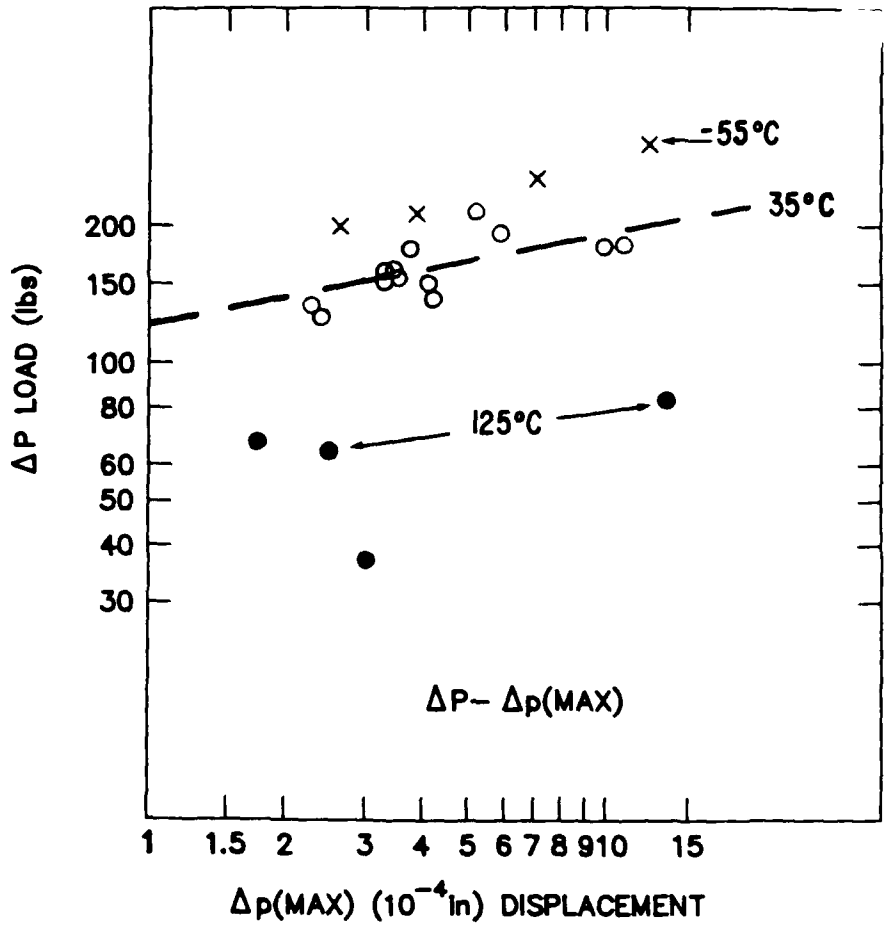

Figure 4. **Hysteresis load range vs. $\Delta_{p(max)}$ for tests at +125 °C and -55 °C compared to the prior results obtained at 35 °C.**

section.

The fatigue cycling resulted in cracking of the solder joints which were detected by a decrease in the load required to produce a given displacement and an increase in the resistance of the joints. This is illustrated in Figures 5 and 6. The load drop is shown as $1 - \left(\frac{\Delta_p}{\Delta_{p\,(max)}}\right)$ so that at the start of the test when the load range Δ_p is equal to the maximum load range $\Delta_p$max, the parameter is 0 and when $\Delta_p \approx 0$ it is 1. The resistance is shown as $(R/R_o/R_D/R_{Do})$-1, where R is the resistance at any cycle and R_o is the initial reference resistance. R_D and R_{Do} are the resistance and initial resistance of a dummy, unloaded, joint which is used to compensate for slight temperature changes which induce resistance changes. The resistance change for three of the joints exhibiting the greatest resistance increase is shown along with the resistance increase of the joint showing the median change and that for the joint showing the least change. The maximum, median, and minimum change curves are labeled Mx, Md, and Mn, respectively.

There is a significant difference between the behavior of specimens tested at -55 °C and 125 °C. While the load drop observed at both temperatures is similar, the resistance increase is not. At 125 °C, a resistance increase begins at the start of the test, but at -55 °C, the resistance does not appear to increase until the load has dropped by about 90% and then increases rapidly for most of the joints.

Figure 7 shows the number of cycles to decrease load by 25% vs. $\Delta_{p\,(max)}$, and Figure 8 shows the same N_f vs. $\Delta_{ps\,(max)}$, as measured on the row of joints which finally failed. These figures show the results at 35 °C as a reference for the data obtained at -55 °C and + 125 °C. The 125 °C data is so close to the 35 °C data that no separate trend line is shown for these points. Two curves are shown for the -55 °C data obtained with both rows of joints. One was obtained using Δ_p and the other with Δ_{pz}. This was done because the loop distortion made these two displacements different even at the start of the test. No correlation is given for Δ_{pz} for the 35 °C or 125 °C data because at these temperatures there was no difference between Δ_p and Δ_{pz} at the start of the test. This was not the case for the -55 °C data, hence the display of the Δ_{pz} data points.

Figures 7 and 8 and subsequent figures show that the fatigue life N_f can be related to the applied displacement, Δ_p, Δ_{ps} or Δ_{pz} by a pseudo Coffin-Manson law, i.e.,

$$N_f^{\alpha}\,\Delta_p = \theta \qquad (1)$$

This is a pseudo Coffin-Manson law because it relates N_f to displacement Δ_p, instead of a strain. The displacement Δ_p can be converted into a strain by dividing by a suitable length. Unfortunately, there is no single length to use because the strain

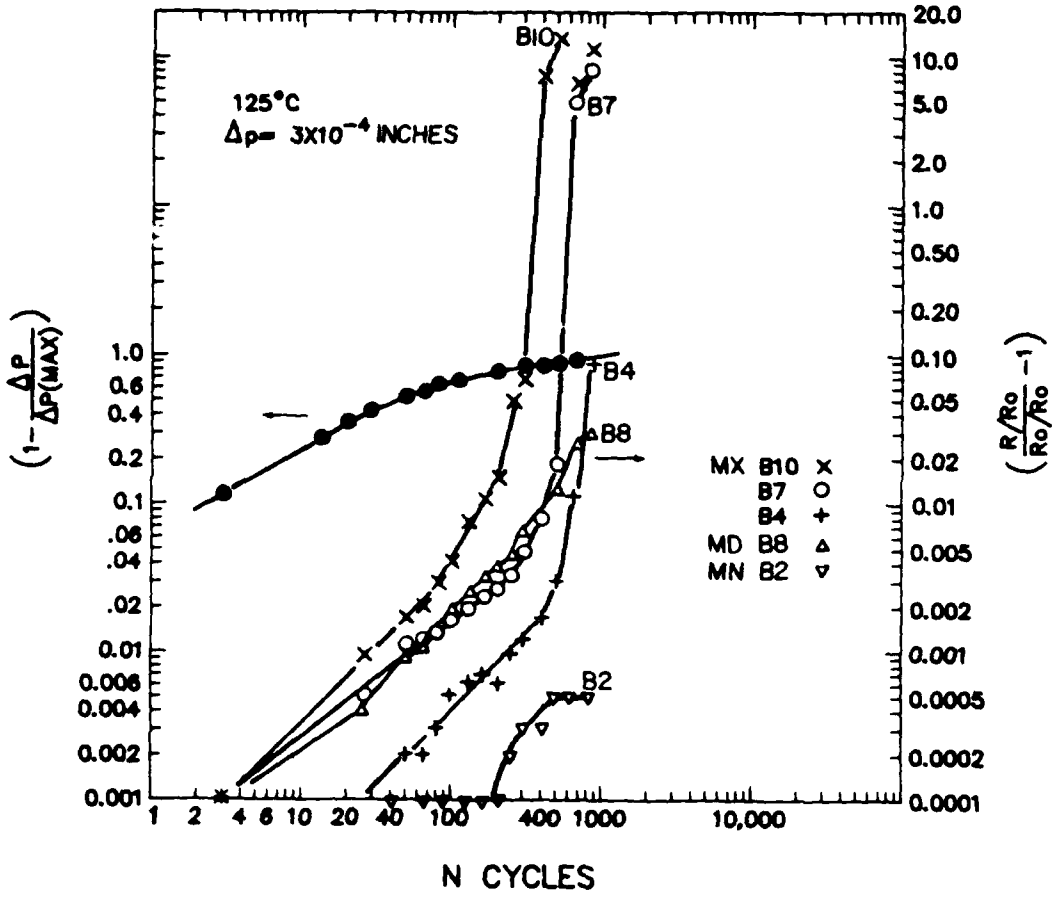

Figure 5. Load drop and resistance increase with cycling at 125 °C.

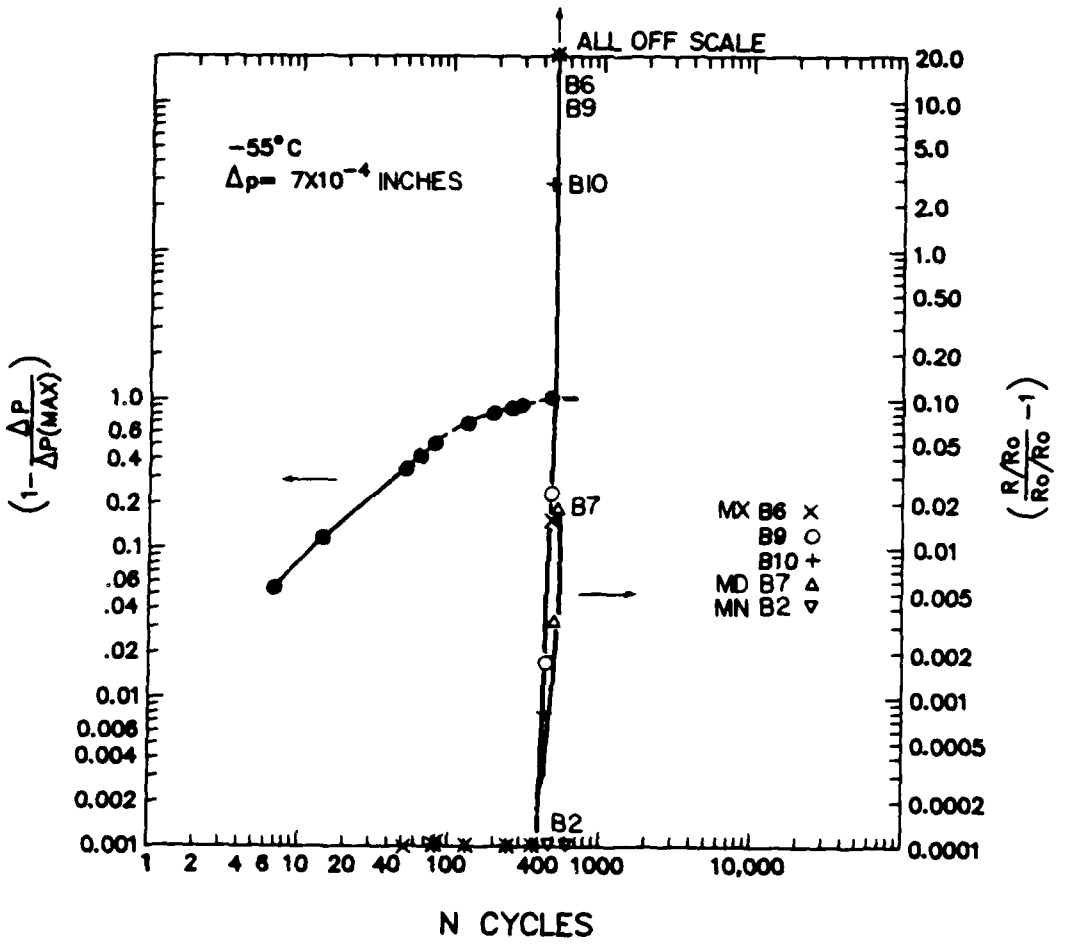

Figure 6. Load drop and resistance increase with cycling at -55 °C.

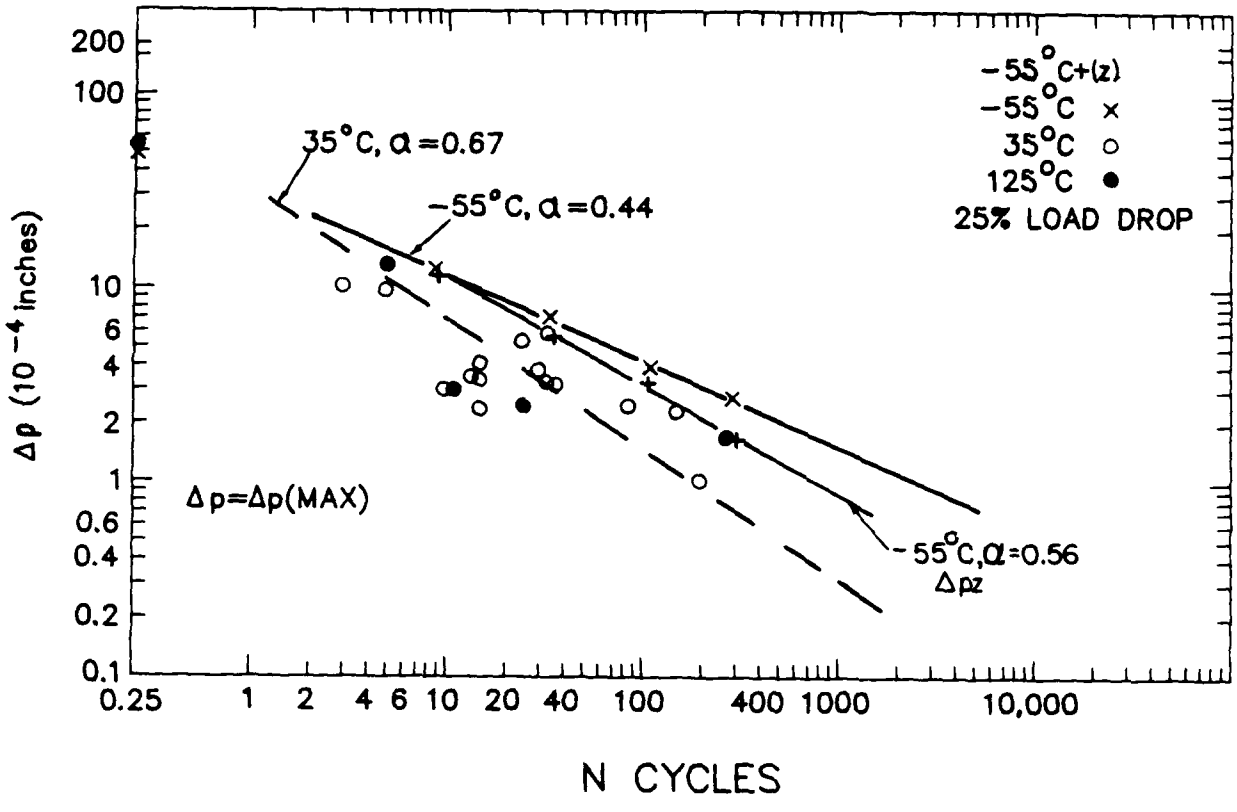

Figure 7. **Displacement vs. N_f for N_f defined by a 25% drop in load. The displacement Δ_p is the sum of that measured for both rows of joints.**

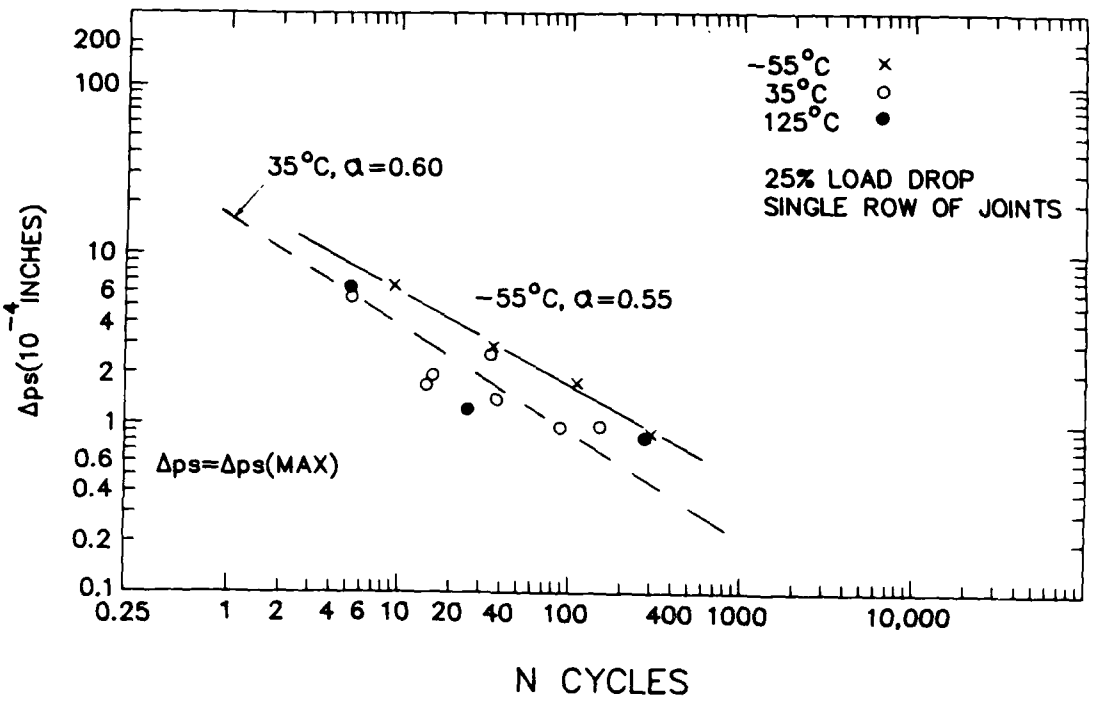

Figure 8. Displacement of a single row of joints, Δ_{ps}, vs. N_f for N_f defined by a 25% drop in load.

distribution is highly non uniform [1]. Nonetheless, N_f can be correlated to Δ_p, so long as consistent definitions for Δ_p and N_f are used.

Figures 9 and 10 are similar to Figures 7 and 8 but were obtained for a 50% drop in load. The displacements are the averages of those measured at the start of the test and when the 50% drop in load was reached. The error bars define these displacements when the difference between the values was larger than the size of the data point. The decrease in displacement with cycling results from a compliance change due to cracking of the joints [1]. No correlation is given for Δ_{pz} for the 35 °C or 125 °C data because at these temperatures there was only a very small difference between Δ_p and Δ_{pz} even when the load dropped by as much as 50%.

The measurement of failure vs. Δ_{ps} as well as Δ_p was done because it tells how the strain is partitioned between the rows of joints and this gives valuable information concerning the failure process [1]. Table 1 lists the ratio of Δ_{ps}/Δ_{pz} vs. the % drop in load at 125 °C, 35 °C and -55 °C. The displacement Δ_{pz} is used rather than Δ_p because Δ_{ps} is measured at zero load so Δ_{pz} should be used because it is also measured at zero load.

Table 1

Load Drop	Initial	50% Load Drop	90% Load Drop
Δ_{ps} / Δ_{pz} At 125 °C	0.49 ± .01	0.54 ± 14	0.80 ± .04
At 35 °C	0.49 ± .07	0.56 ± .12	0.75 ± .14
At -55 °C	0.54 ± .02	0.67 ± .02	0.83 ± .09

Table 1 shows that, on the average, the strain is initially partitioned roughly equally between the rows of joints, but that as the test progresses, the displacement becomes concentrated in one row. This concentration is due to the development of fatigue cracks. When the cracking in one row gets ahead of that in the other, it weakens that row and causes more of the deformation to occur in that row. Since the control is on the sum of the displacements of both rows, if more displacement occurs in one row, less will occur in the other. The more one row deforms relative to the other, the more cracking will take place and the more this will further concentrate the displacement. This also has the effect of retarding or even stopping cracking of joints in the other row of joints [1].

Figures 11 and 12 show N_f for a 90% drop in load correlated with the sum of the displacements measured across both rows and with the displacement measured across

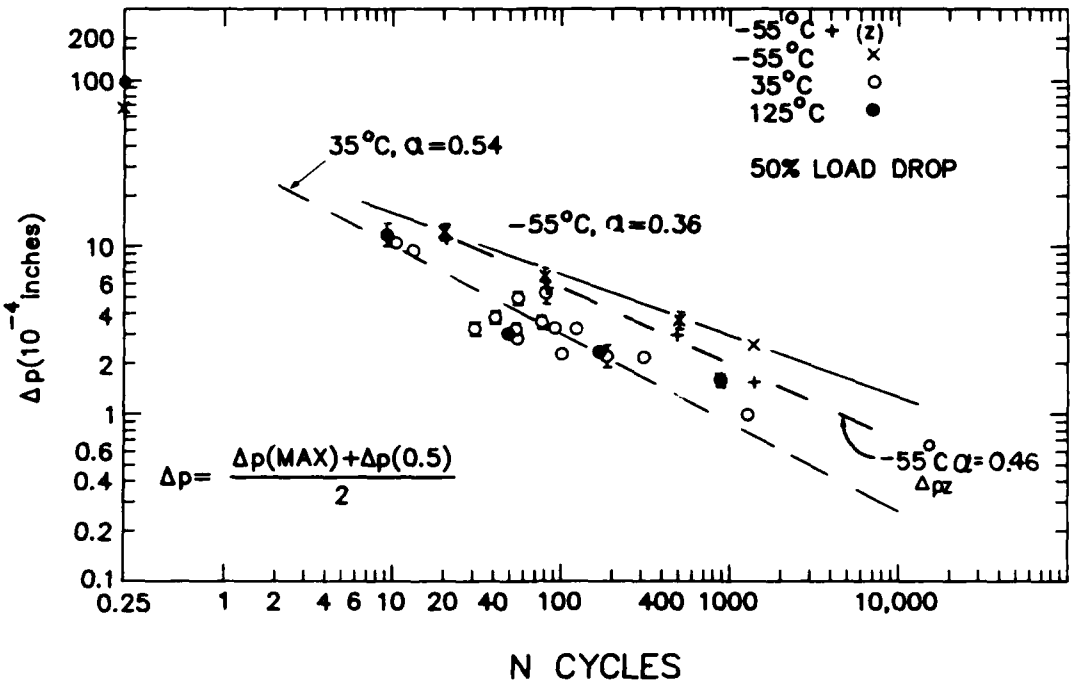

Figure 9. Displacement (sum for both rows) vs. N_f for N_f defined by a 50% drop in load.

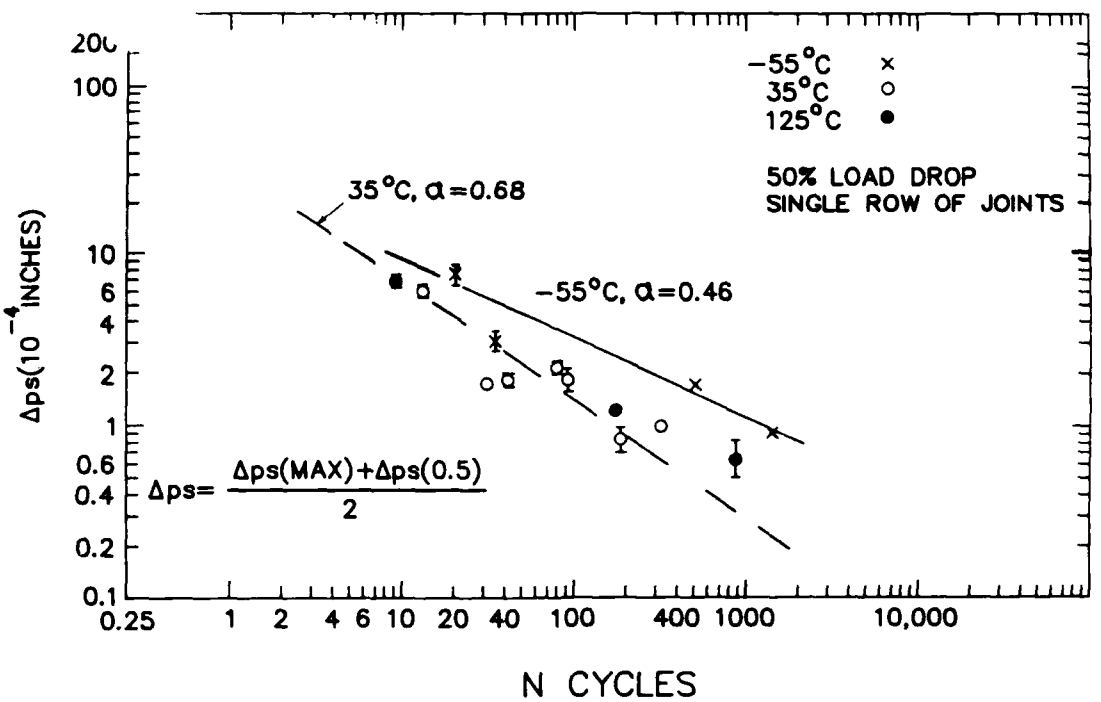

Figure 10. Displacement of a single row of joints vs. N_f for N_f defined by a 50% drop in load.

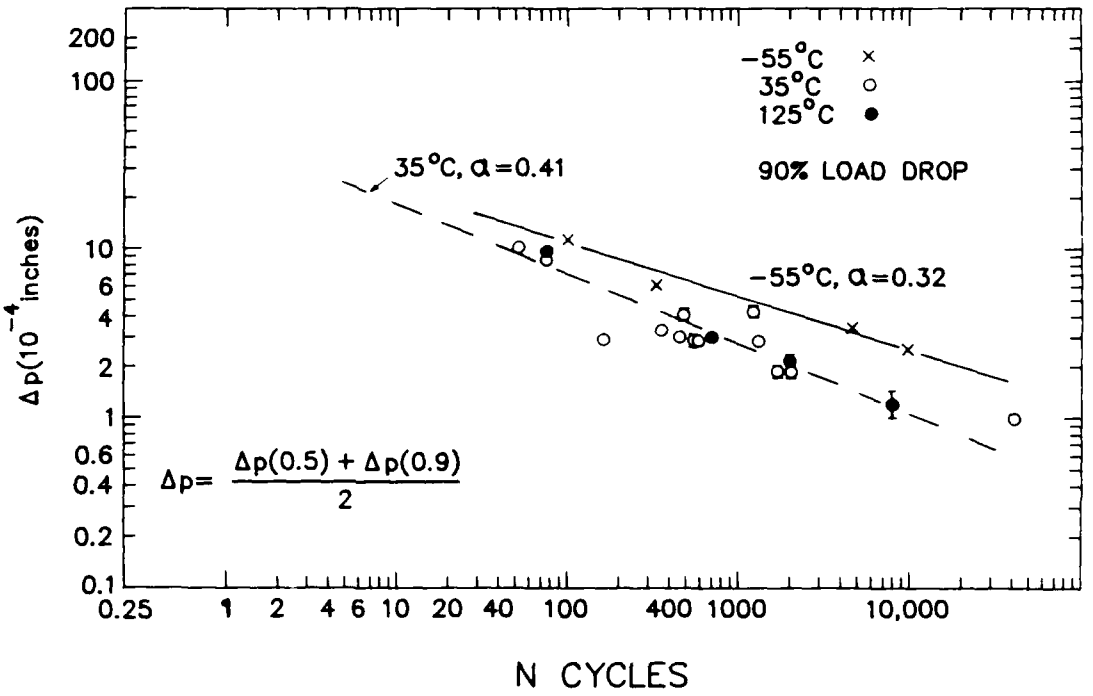

Figure 11. **Displacement (sum for both rows) vs. N_f for N_f defined by a 90% drop in load.**

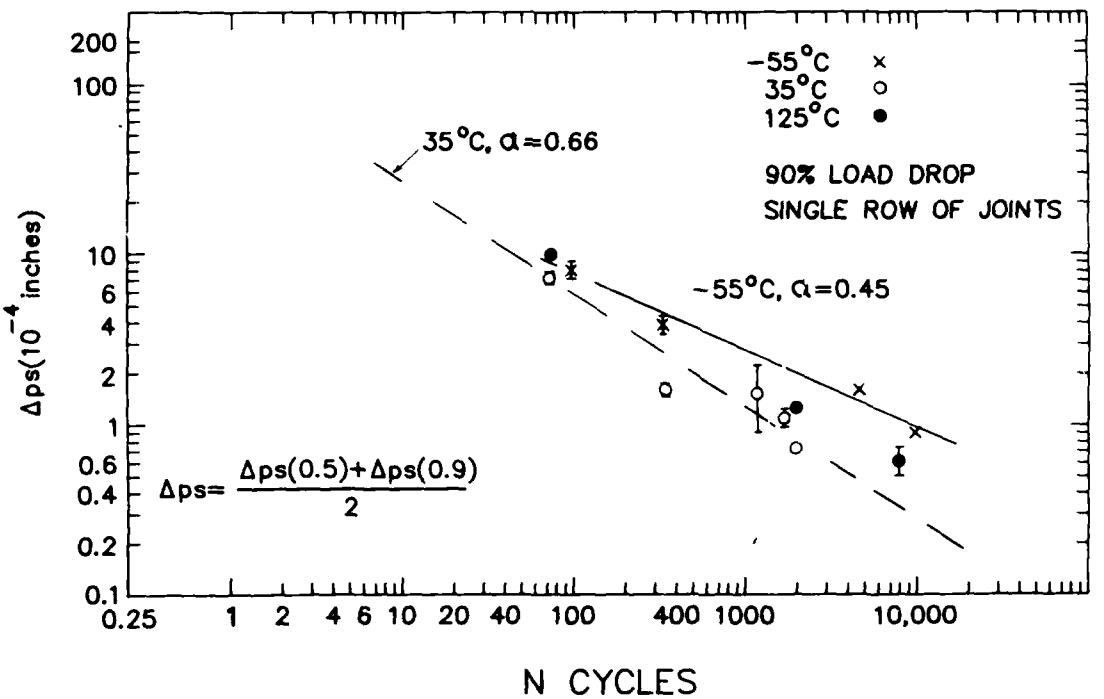

Figure 12. **Displacement of a single row of joints vs. N_f for N_f defined by a 90% drop in load.**

a single row. Here, the average of $\Delta_{p\,(0.5)}$ and $\Delta_{p\,(0.9)}$ (or $\Delta_{ps\,(0.5)}$ and $\Delta_{ps\,(0.9)}$) is being used. This average rather than the average from $\Delta_{p\,(max)}$ was used because relatively little of the fatigue life is spent in decreasing the load in half, so using the displacement in the interval from $\Delta_{p\,(max)}$ to $\Delta_{p\,(0.5)}$ would cause an overestimate of the actual displacement operating through most of the test (i.e., the interval between the 50% drop in load and the 90% drop in load). The error bars define the extremes in the displacements between $\Delta_{p\,(0.5)}$ and $\Delta_{p\,(0.9)}$.

Figures 13 and 14 show N_f as determined by extrapolation to a 100% drop in load vs. $\Delta_{p\,(0.9)}$. The displacement measured at the 90% drop in load was utilized because this is the displacement operating during the final stages of the test. The slow drop in load means that N_f for 100% failure is roughly twice as long as that required to reduce the load by 90%. This displacement measured at the 90% drop in load more accurately reflects the displacement than if an average over the entire test were used.

Figures 7-14 show that not only is the fatigue life somewhat longer at -55 °C than at 35 °C or 125 °C, but the slope of the curve, α, is lower. Some of the difference in α, when Δ_p is used to correlate the data, is due to the hysteresis loop distortion. When Δ_{pz} is used, α is increased to close to that observed at the higher temperatures. In general, there was less of a difference in α when the single joint data was considered (see Figures 7, 9, 11, and 13) because Δ_{ps} like Δ_{pz} is measured at zero load and more accurately reflects the plastic strain when there is hysteresis loop distortion, as there is at -55 °C.

While Δ_p is equal or almost equal to Δ_{pz} at 35 °C and 125 °C for the early part of the test, this is not true when the load drops to 90% or more [1]. This change is due to an increase in the compliance caused by cracking. At -55 °C there is a decrease in Δ_{pz} due to this compliance change which adds to the decrease due to the hysteresis loop distortions that have already been mentioned. The correlations with Δ_{pz} for a 90% and 100% drop in load are shown in Figures 15 and 16. Once again, utilizing Δ_{pz} has the effect of increasing α because the decrease in displacement (i.e., Δ_{pz} compared to Δ_p) is proportionally greater at low strains than at high strains.

Figures 17-23 show the fatigue life as defined by increases in resistance of the joints showing the largest resistance increase. Figure 17 shows N_f defined by a 0.02% increase in resistance, which is the smallest increase in resistance that was considered. As can be seen, and as will be discussed, the number of cycles to produce this small resistance increase is much greater at -55 °C than at higher temperatures. The lives are longer because the load drop required to produce such a resistance increase was about 80% at -55 °C compared to about 25-40% at higher temperatures (see the legend of this and the subsequent figures for this data).

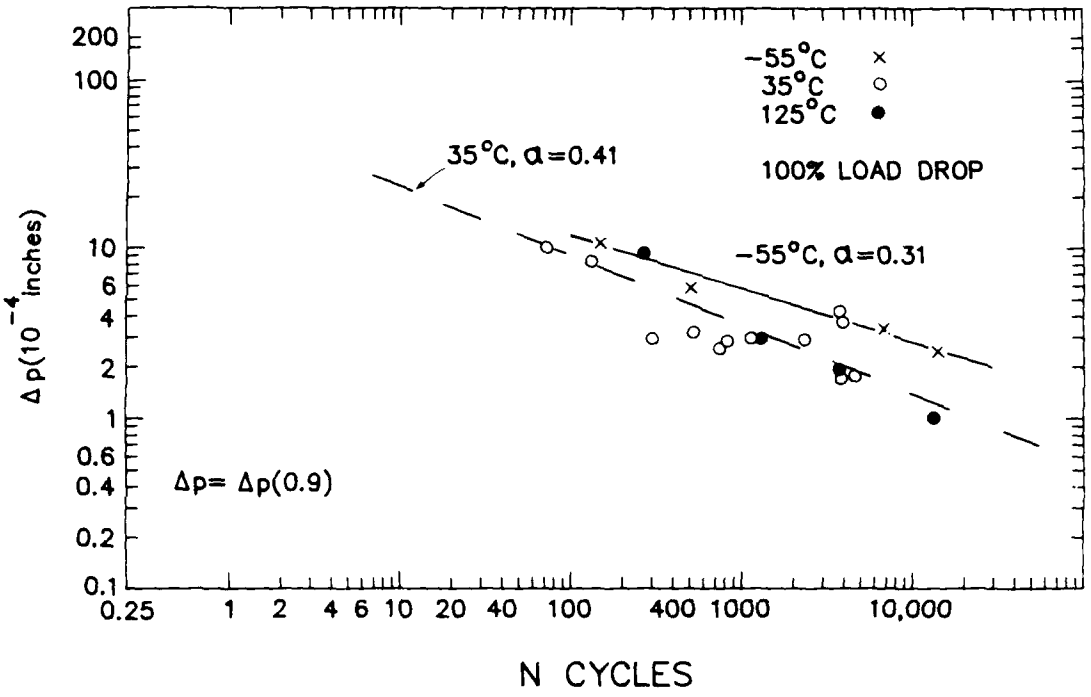

Figure 13. **Displacement (sum for both rows) vs. N_f for N_f defined by an extrapolation to a 100% drop in load.**

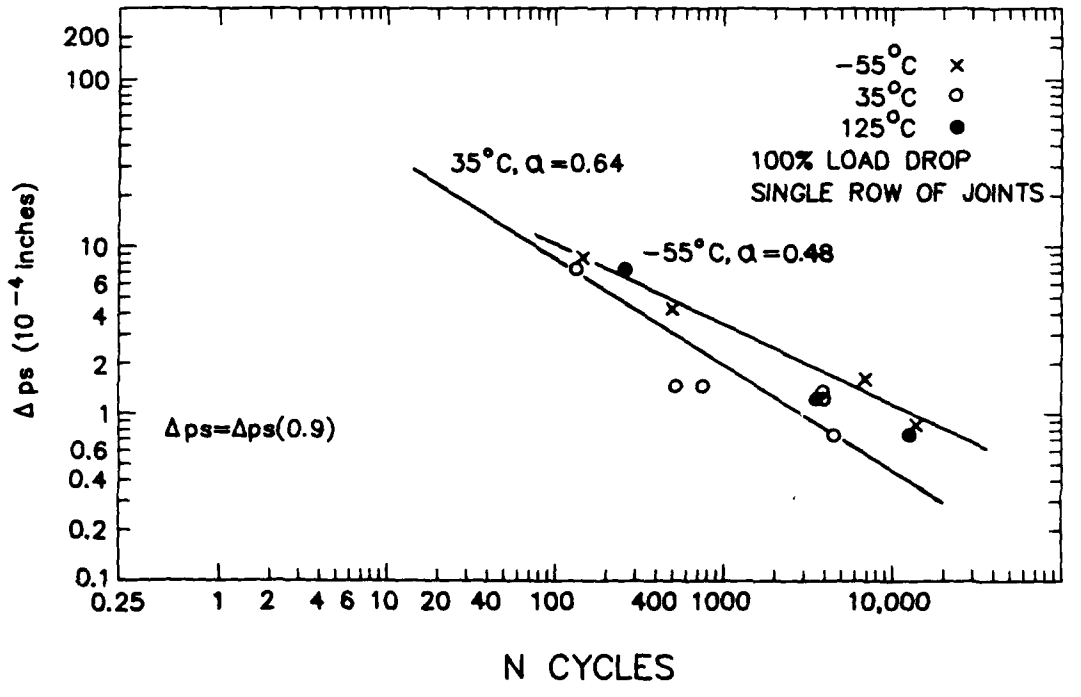

Figure 14. **Displacement of a single row of joints vs. N_f for N_f defined by an extrapolation to a 100% drop in load.**

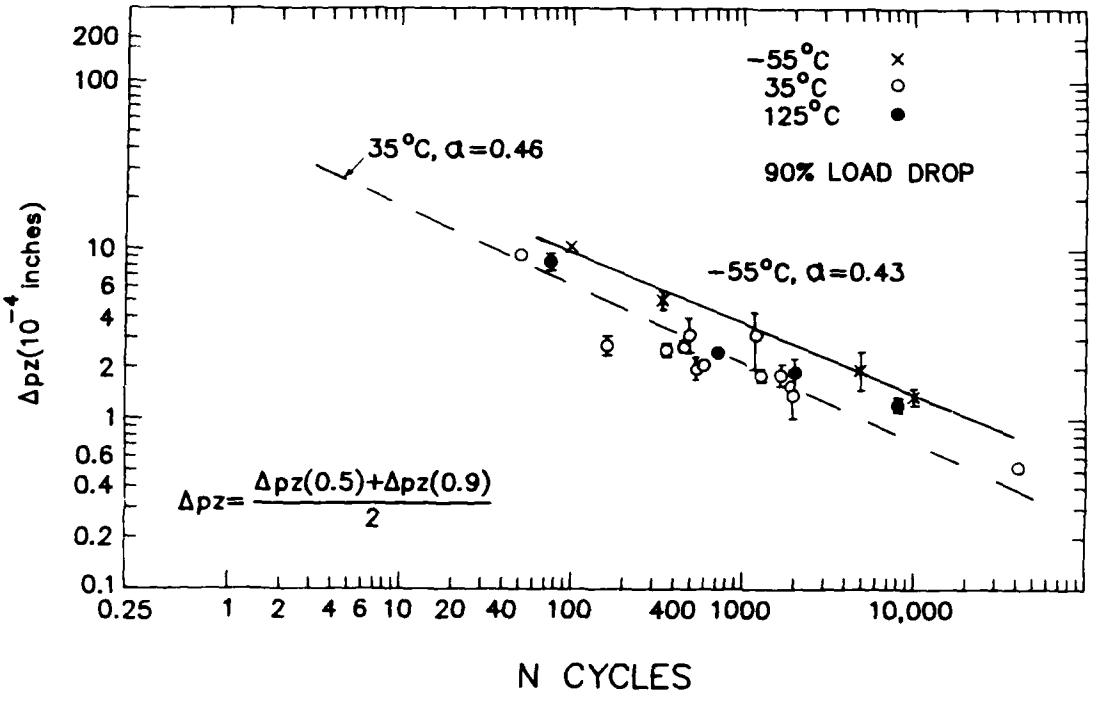

Figure 15. Displacement measured at zero load, Δ_{pz}, vs. N_f for a 90% decrease in load.

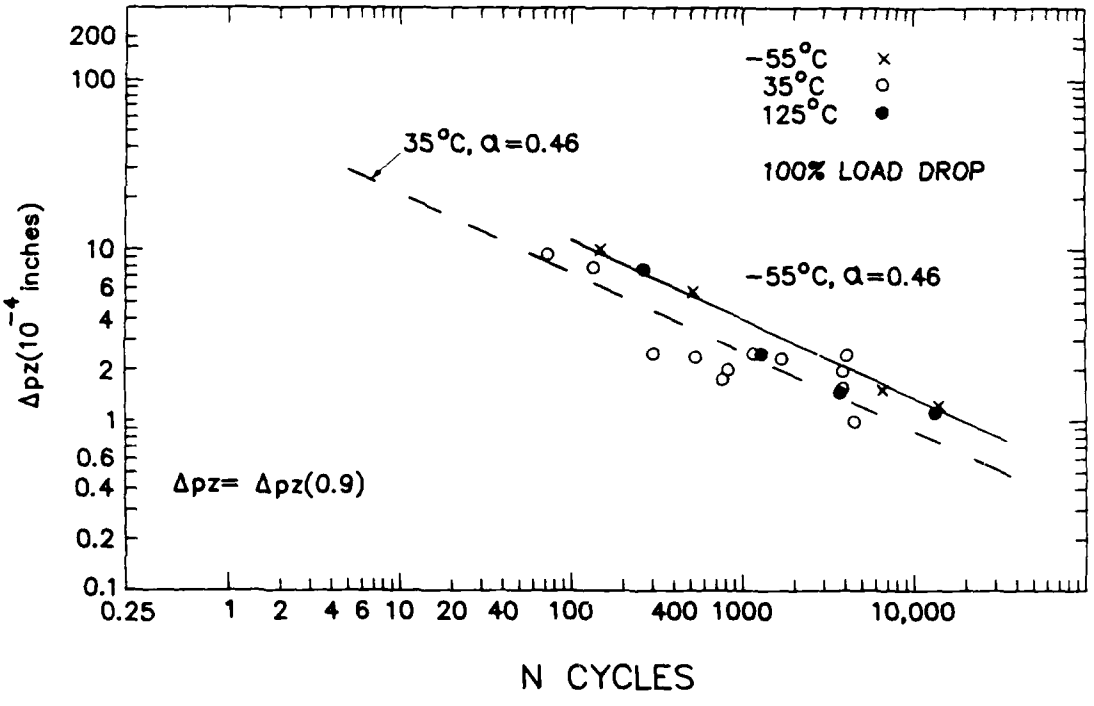

Figure 16. Displacement measured at zero load, Δ_{pz}, vs. N_f for a 100% decrease in load.

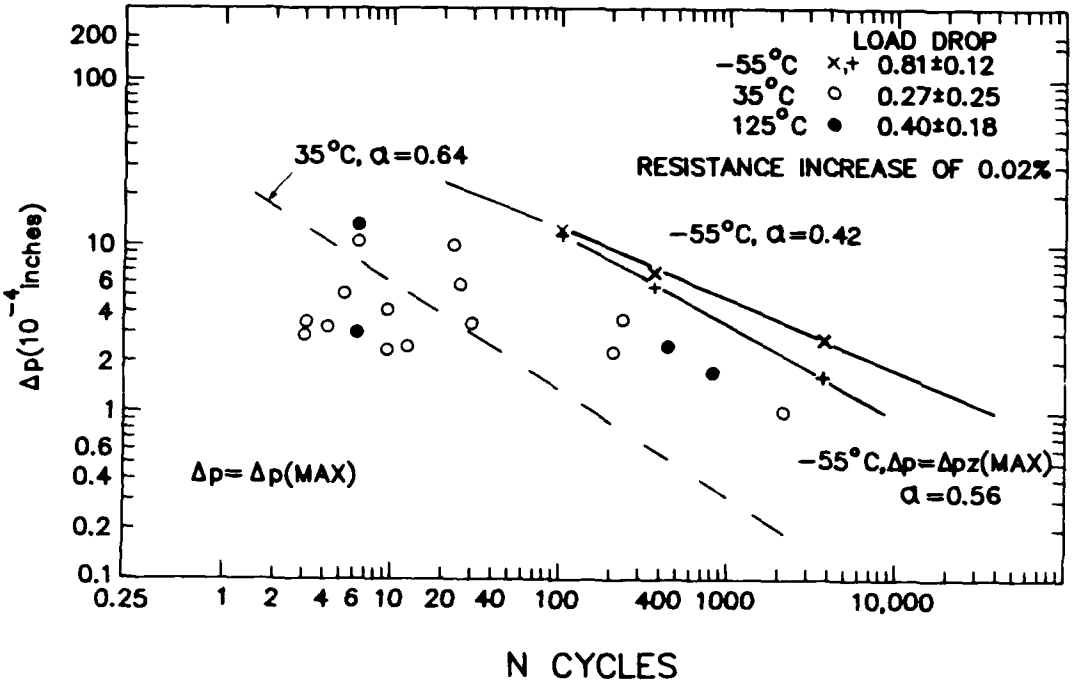

Figure 17. **Displacement vs. N_f for N_f defined by the first joint to experience a 0.02% resistance increase.**

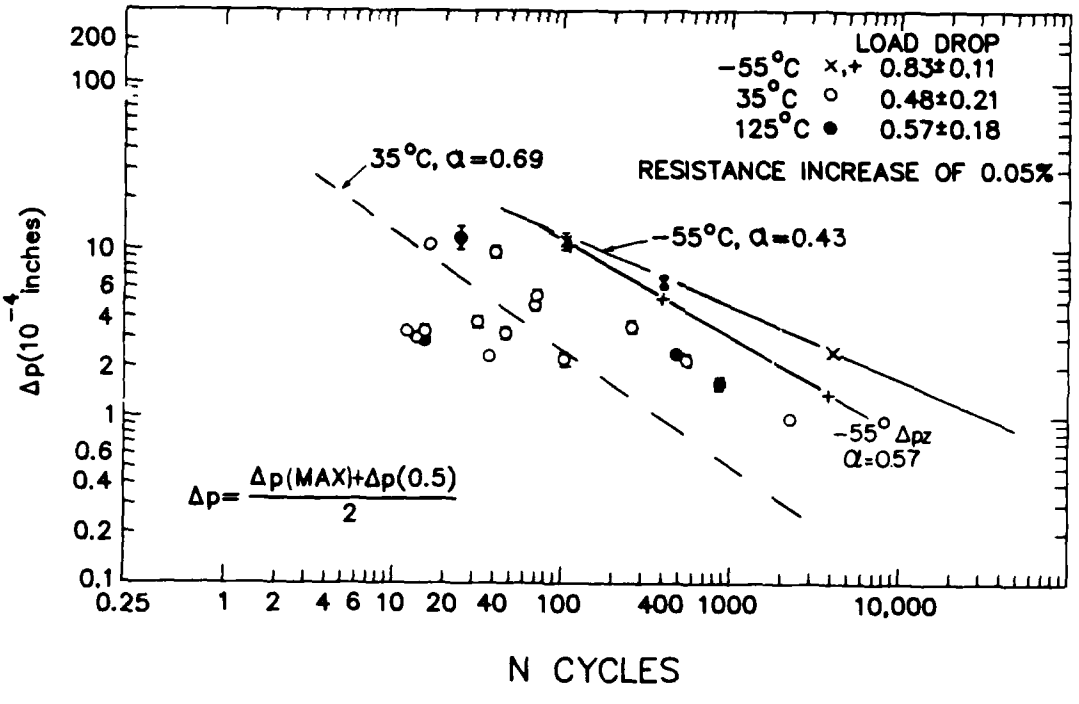

Figure 18. **Displacement vs. N_f for N_f defined by the first joint to experience a 0.05% resistance increase.**

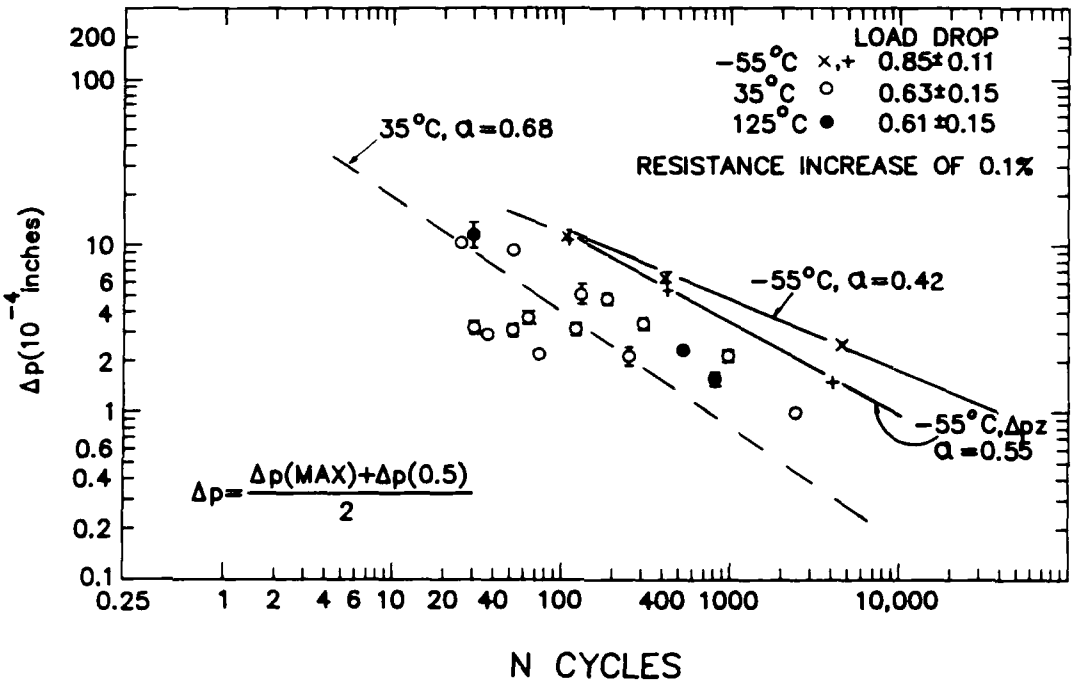

Figure 19. **Displacement vs. N_f for N_f defined by the first joint to experience a 0.1% resistance increase.**

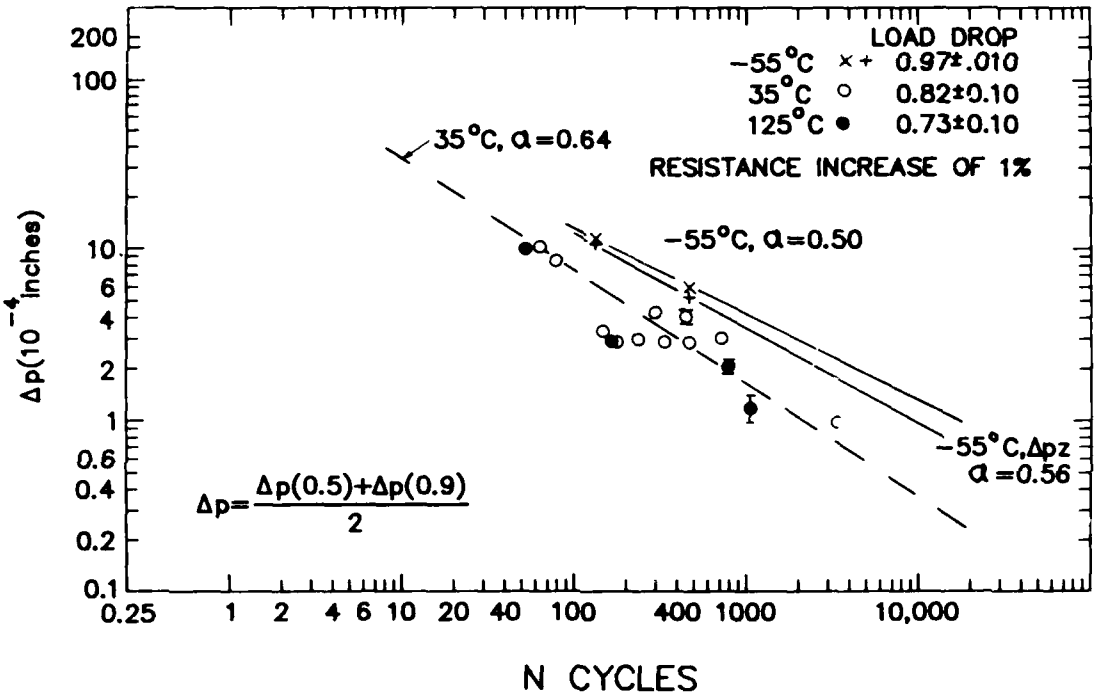

Figure 20. **Displacement vs. N_f for N_f defined by the first joint to experience a 1% resistance increase.**

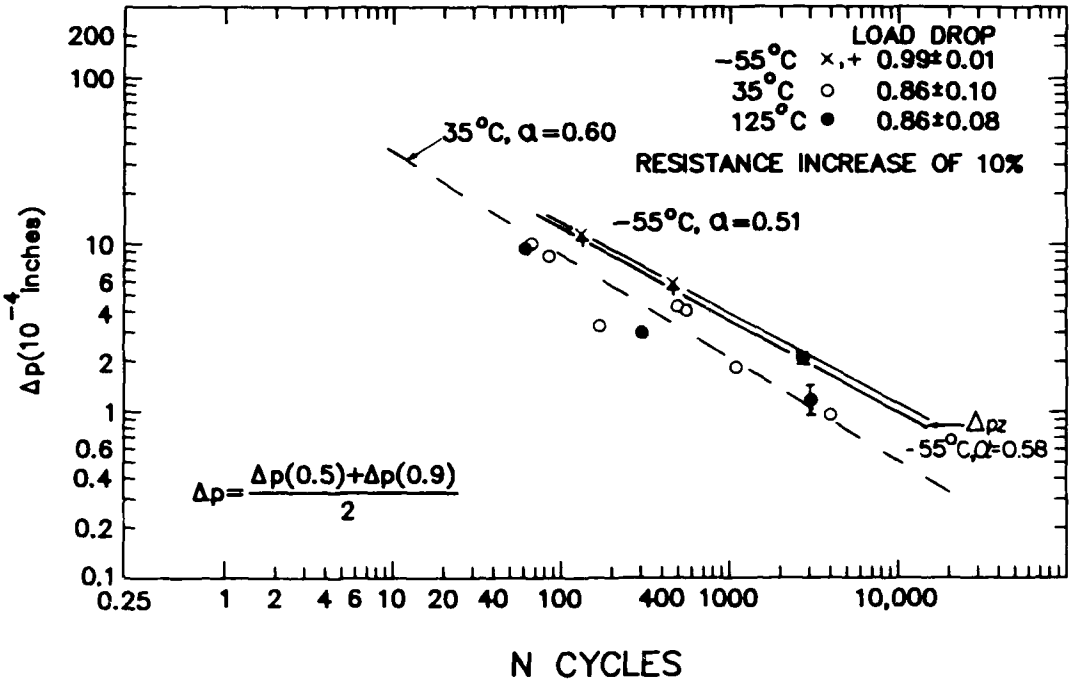

Figure 21. **Displacement vs. N_f for N_f defined by the first joint to experience a 10% resistance increase.**

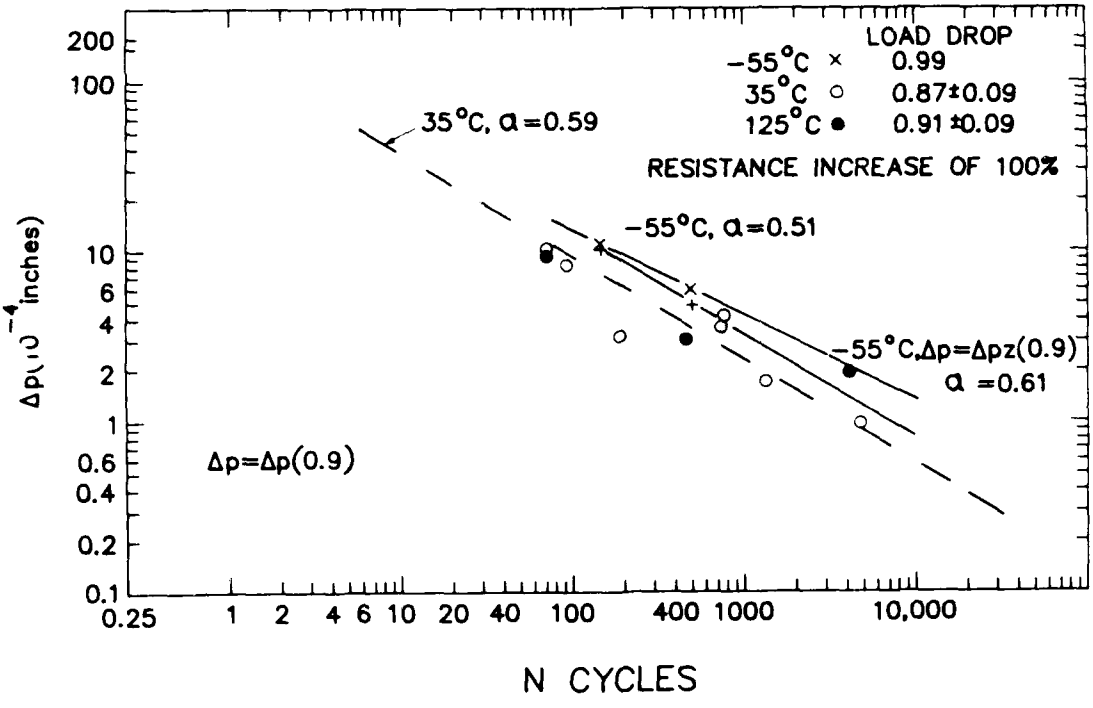

Figure 22. **Displacement vs. N_f for N_f defined by the first joint to experience a 100% resistance increase.**

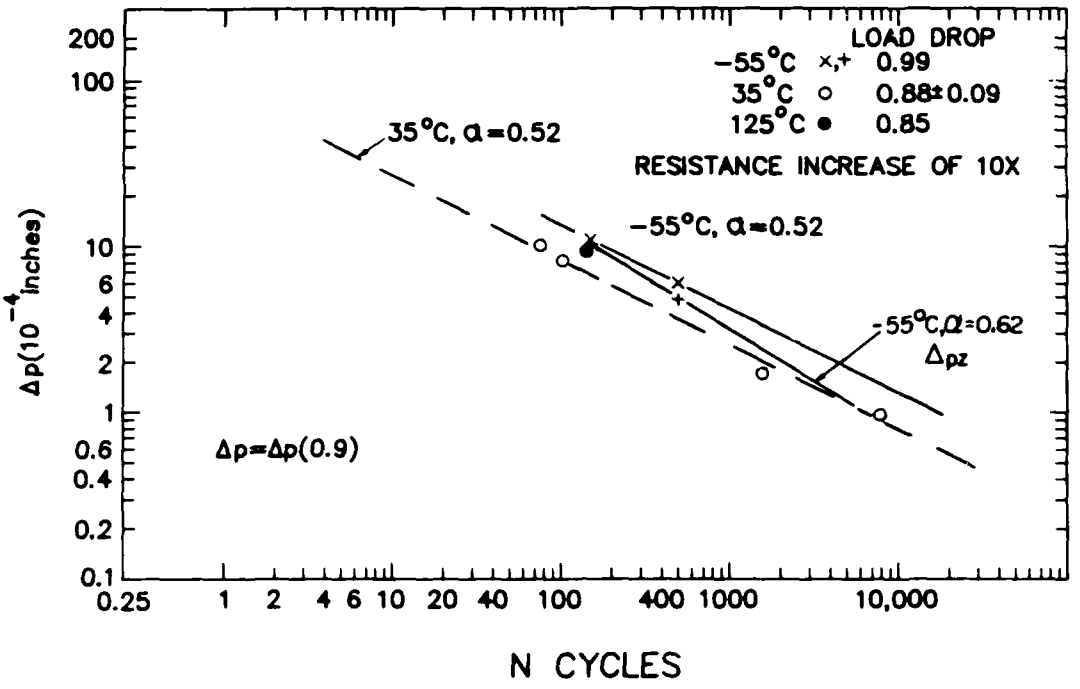

Figure 23. **Displacement vs. N_f for N_f defined by the first joint to experience a 10X resistance increase.**

Figures 18-23 are similar to Figure 17 in that the number of cycles to raise the resistance by 0.05%, 0.1%, 1%, 10% or 100% is greater than at higher temperatures. Furthermore, in agreement with the data of Figure 17, the load drop required to reach this resistance increase was greater at -55 °C than at higher temperatures. This difference decreases, however, as the test progresses as does the difference in N_f.

Figures 17-23 show the -55 °C resistance data in terms of the displacements measured at zero load, as well as at the load reversal. As with the load drop data, using a zero load definition for the displacement raises α and brings the 55 °C data more in line with the α measured at the higher temperatures.

4. DISCUSSION

The results of the preceding section conform to the model for joint fatigue failure discussed in Ref. 1. In that study, cross sections of joints which were cycled to a 30% or 60% drop in load were studied along with the fillets in joints cycled to larger drops in load. These observations were used to develop the following model for joint failure. The initial drop in load results from cracking beneath the chip carrier, but this gives rise to very little change in resistance. The load must drop to greater than 50% before cracks can be observed in the fillets of some joints and the resistance is increased to greater than 0.1%. Further cycling enlarges these cracks and causes other joints to exhibit cracks.

The behavior at 125 °C is the same as that at 35 °C. The 125 °C low cycle fatigue data falls within the scatter in the 35 °C data and the correlation of the drop in load with the resistance increase is similar; thus no attempt has been made to separate the 125 °C results from those obtained at 35 °C.

At -55 °C, the general behavior is similar to that observed at the higher temperatures, except for the fact that the lives are longer and the load has to drop by greater than about 80% before any resistance increase is noted. This behavior may be due to current passage through the crack faces making it appear, electrically, that the joint is uncracked. In these shear tests, the faces do not separate as they do when a tensile load is applied. Oxidation and local deformation of high points will prevent current passage across a shear crack. These factors are reduced when the temperature is reduced (i.e., there is less oxidation and the solder is stronger, so there may be less local deformation). Thus, at -55 °C, it is more difficult to produce a resistance increase, even when the joint is cracked. This is illustrated in Figure 24, where cracks are visible in the fillet of joint T11, T10, and T7 even though no resistance increase was observed. This specimen was cycled to a load drop of 65%, which is a level which also produces cracks at 35 °C and 125 °C, but at these higher temperatures this cracking produces resistance increases of 0.1% or greater. In the case of a crack as large as that shown in joint T11 (Figure 24a), a resistance increase of greater than 1% would

(a)

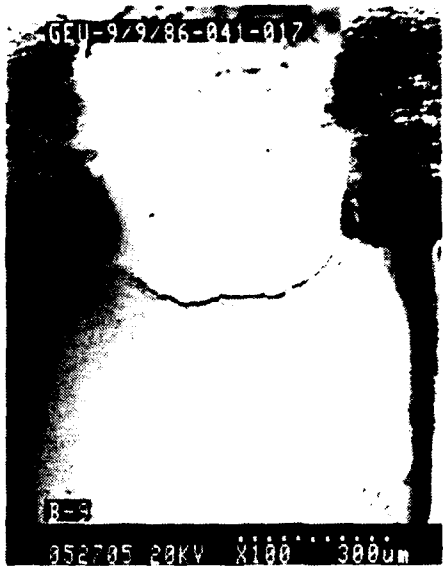

(b)

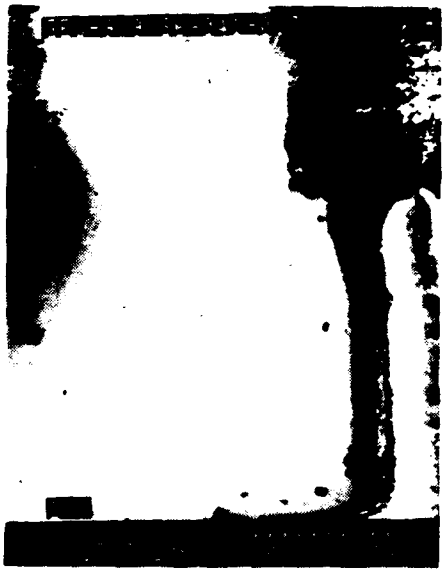

(c)

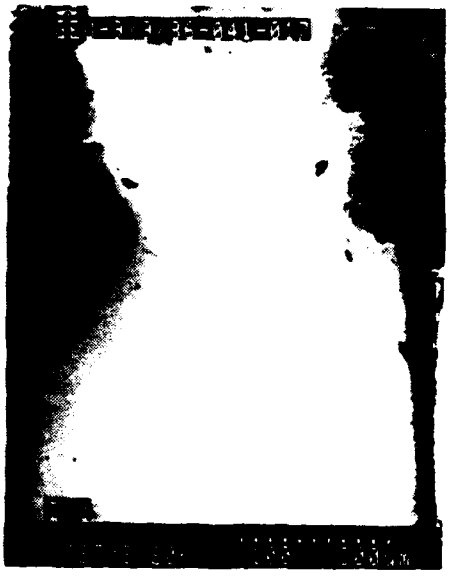

(d)

Figure 24. **Joints in a specimen cycled at -55 ℃ to a load drop of 66%. a) Joint T11, b) Joint T10, c) Joint T7, and d) Joint T1.**

be expected at 35 °C or 125 °C.

Another feature which distinguishes the -55 °C data from the 35 °C or 125 °C data is the generally lower slopes (α) of the Δ_p vs. N_f curves. This is a result of the hysteresis loop distortion, shown in Figure 3, which develops at -55 °C, especially as the load decreases and the compliance increases. As is shown, this distortion does not develop at 125 °C, partially because of the low loads required to produce deformation and therefore smaller influence of the compliance increase. Because of this distortion, it is more appropriate to use Δ_{pz} instead of Δ_p in correlating the -55 °C displacements with the fatigue life. As Figures 9, 11, and 13 show, when $\Delta_{p(z)}$ is used to define the imposed plastic displacement, there is much better agreement between α measured at 35 °C, 125 °C and -55 °C.

The large differences between Δ_{pz} and Δ_p at -55 °C, shown in Figure 3, reflect the fact that the compliance has changed appreciably, but such changes have not been incorporated by the plastic strain computer. The net result is that the plastic strain being applied is reduced, and since it is this plastic strain which causes the fatigue failure, it is important to correlate the fatigue life with Δ_{pz}. The single row of joint data also uses the displacement at zero load, hence the reasonably good agreement in the high and low temperature measurements of α, which is higher than that measured with Δ_p for both rows because of the compliance changes with cycling [1].

The less the actual plastic deformation that develops in the joints, the longer will be the fatigue life. If joint bending rather than straining occurs, then much of the displacement will not be effective in producing displacements and the resulting fatigue cracks. In the extreme, joint bending might accommodate all the imposed displacement (i.e., zero displacement width hysteresis would develop). At elevated temperatures, this sort of joint bending is not as large because the flow stress is lower and creep rapidly relieves any joint bending stresses. Even at 35 °C and 125 °C, there is still, however, some compliance change with cycling because the area of the joint is reduced by fatigue cracking. This reduces Δ_{pz} but the effect is much less than is observed at -55 °C. The compliance changes are, however, large enough at a 90% drop in load (or extrapolating to 100% drop in load) to use Δ_{pz} to correlate the data at 35 °C and 125 °C as well as at -55 °C. At the higher temperatures, however, the effect is small and α is altered only slightly.

In correlating this data with other data, it is important to use the same basis for comparison. The best basis is to use the data which employs the best definition of plastic strain. The plastic strain reflects the solder behavior. Displacement definitions which include elastic displacements present problems since they incorporate elastic machine displacements and elastic bend displacements, which vary from experiment setup to setup, and with respect to actual CC/PWB joints [2]. For this reason the Δ_{pz} data is used for these correlations.

Table 2 compares α as a function of temperature for a 50% drop in load, for this study and for tests [3,4] run on single, 0.0075 in. thick, joints which did not have fillets. These single joints were 0.1 x 0.5 in. and thus had an area which was roughly equal to that of the multiple joints tested here. With this simple joint geometry, it was possible to calculate $\Delta\gamma_p$ by dividing the displacement by the joint thickness. This cannot be done for the joints tested here because of the extensive strain gradients developed in the fillet. Nonetheless, it is possible to compare these two data sets, at least as far as the slope α is concerned. The intercepts are, however, quite different and reflect the the fact that in previous tests strains are used instead of displacement. Dividing the displacement by an appropriate length will convert it to a strain and shift the life curve up or down, but it will not influence the slope α.

The displacement Δ_{pz} was used for the -55 °C tests of this study. Otherwise, since loop distortions were not significant with the simple solder pads or in the current study at 35 °C or 125 °C, Δ_p was used to define the plastic displacements. In the previous study, the low temperature tests were run at -50 °C, but the 5 °C difference should not influence α. As can be seen with a proper definition of Δ_p, there is quite good agreement between α as measured in the various tests.

Two single pad values for α are shown in Table 2. Since it is standard to employ N_f as the abscissa, and Δ_p or $\Delta\gamma_p$ as the ordinate, the least squares fit in Reference 4 was done with this convention. This meant that N_f was being treated as the independent variable instead of the dependent variable, and this introduces an error in the least squares fit to determine α. With N_f as the dependent variable [5], there is a slightly different curve fit, and a different α value is determined (the second column). When there is very little scatter, such as at -50 °C, there is little or no difference in the curve fit and α is not influenced. When there is more scatter, α is different. It should be kept in mind, however, that all the α values are within a 95% probability band. (The present study utilizes the correct curve fit procedures and should therefore be compared with the second column of the single pad results).

Table 2

Coffin-Manson Exponent α for a 50% Drop in Load

Temperature	Single Pads	Present Study
-55 °C (-50 °C)	0.5,0.49	0.46
+35 °C	0.52,0.59	0.54
+125 °C	0.51,0.58	0.54

The fact that the previous study utilized plastic strains rather than plastic displacements, and the difference in the geometry of the joints, prevent a direct comparison of the actual fatigue lives. Relative comparisons are, however, possible. In the previous study [3], it was found that the fatigue life at -50 °C was 1.5 times greater than that observed at 125 °C and scatter of the 35 °C data was large enough that it encompassed the -50 °C and + 125 °C results. In the present study, the fatigue life at -55 °C was generally beyond the scatter band of the 35 °C data. Using the Δ_{pz} data (Figure 16), N_f at -55 °C was about 3.5 times larger than that observed at 35 °C or 125 °C (Figure 9). Considering the difficulties in defining the displacements at -55 °C, and the relatively little data obtained at -55 °C or + 125 °C, the agreement between this study and the previous one is reasonable.

5. CONCLUSIONS

1. Low cycle fatigue data obtained on CC/PWB joints at -55 °C, +35 °C and + 125 °C is similar to that observed in previous LCF tests on single solder pads.

2. A load drop of 80% was required before a resistance increase was observed at -55 °C. In contrast, at 35 °C or 125 °C, resistance increases of 0.1% or more were noted when the load dropped by as little as 60%. At a 66% load drop at -55 °C, no resistance was noted even though cracks in the fillets were clearly observed after the test. It is believed that this behavior results from more shorting across the crack faces at -55 °C than at higher temperatures.

3. The hysteresis loops were distorted at -55 °C. This prevented the plastic strain measured at the cross head reversals from giving an accurate correlation of the data. Instead, the plastic strain measured at zero load was successfully employed.

ACKNOWLEDGMENTS

The author gratefully acknowledges fruitful discussions with John DeVore (GE E Lab, Syracuse), Bill McFarland, GE-CRD, Walt Pillar (GE-AESO, Utica), and Bill Fahy (GE-AESD, Utica).

This work was performed under AF Contract #F33615-85-C-5065. The author is grateful for this support and for the support given by Don Knapke, Preston Opt and Ed Morrisey, all of the AF Materials Lab (WPAFB, Ohio).

REFERENCES

[1] H.D. Solomon, "Low Cycle Fatigue of Surface Mounted Chip Carrier/Printed Wiring Board Joints," GE internal report 87CRD185, September 1987.

[2] H.D. Solomon, "Low Cycle Fatigue of 60/40 Solder-Plastic Strain Limited vs. Displacement Limited Testing" in Electron Packaging: Materials and

Processes, Ed. J. A. Sartell, ASM 1986, pp. 29-49.

[3] H.D. Solomon, IEEE – CHMT-9, pp. 423-433 (1986).

[4] H.D. Solomon, to be published.